Paper No.
2686

NACE INTERNATIONAL CORROSION 2013 CONFERENCE & EXPO

Investigation of Stress Corrosion Cracking Susceptibility of High Strength Stainless Steels for Use as Strand Material in Prestressed Concrete Construction in a Marine Environment

Joseph Fernandez
University of South Florida
4202 East Fowler Ave
Tampa, Florida 33784
USA

Alberto Sagüés
University of South Florida
4202 East Fowler Ave
Tampa, Florida 33784
USA

Gray Mullins
University of South Florida
4202 East Fowler Ave
Tampa, Florida 33784
USA

ABSTRACT

Stainless steel reinforcing has an elevated chloride threshold and is an attractive alternative for prestressed concrete applications. However, due to the high strength requirements for prestressing strands, concern exists about the possibility of stress corrosion cracking (SCC). This investigation screened for potential SCC development three candidate high strength alloys for use as prestressed strands in a Florida marine environments. The alloys were a common austenitic stainless steel with high nickel content UNS[(1)] # S31603, a less common austenitic stainless steel with low nickel but high manganese UNS# S24000, and a duplex stainless steel with high chromium and an additional constituent, molybdenum UNS# S32205. The alloys were evaluated at various temperatures in $MgCl_2$ solutions and also in a simulated concrete pore water solution at 60 ^{o}C, followed by an anodic polarization regime as an alternative test acceleration method. The results suggest that duplex high-strength stainless UNS# S32205 performed overall better than the other two alloys.

Key words: Magnesium Chloride, Relative Humidity, High-Strength Steel.

[(1)] Unified Numbering System for Metals and Alloys (UNS). UNS numbers are listed in *Metal & Alloys in the Unified Numbering System,* 10th ed. (Warrendale, PA: SAE International and West Conshohocken, PA: ASTM International, 2004).

INTRODUCTION

The service life of prestressed concrete piles is, in part, dictated by the time required to corrode the steel once chloride ions are at the surface of the steel.[1,2] Therefore, by increasing the chloride threshold of the steel an increased service life can be expected. Stainless steel reinforcing has an elevated chloride threshold and is an attractive alternative for prestressed concrete applications. However, due to the high strength requirements for prestressing strands, concern exists about the possibility of stress corrosion cracking (SCC). This investigation screened for potential SCC development three candidate high strength alloys for use as prestressed strands in a Florida marine environments.

Each alloy was subjected to two stress conditions (phases) imposed by varied mechanical fixtures then subjected to various forms of high chloride concentrations. The pH of these conditions was also varied and in one case simulated the high pH common to concrete pore water solutions. Polarization of each alloy to up to 400 mV versus Saturated Calomel Electrode (SCE) above the open circuit potential (OCP), after ~2160 hours, while in a high pH solution categorized the relative passivation range of the alloys.

BACKGROUND

Wu and Nürnberger studied SCC in high-strength stainless steels for use in prestressed concrete structures.[3] Their work focused on the 300 series austenitic stainless steel alloys cold-worked to high-strength. Partial testing of a duplex stainless steel was also included, but no manganese substitute stainless steel alloy was considered. The austenitic alloys (UNS #S30400, S31600, S31653, and S31753) were tested at three pH regimes (4.5, 8.5, and 12.1) at temperatures from 30 ^{o}C to 80 ^{o}C. During those tests, SCC occurred in all of the steel alloys at 80 ^{o}C at all pH conditions. At 60 ^{o}C, only UNS# S30400 and S31600 experienced SCC within 20,000 hours and in the case of UNS# S31600, this was only at pH 4.5. Increased susceptibility to SCC occurred when either the pH was decreased, or the temperature was increased. UNS# S31753 performed better than the other alloys. The authors also evaluated prestressed piles fabricated using strands made of UNS# S31600, S31653, and S31753 alloys. The testing time in concrete with chloride solution added onto the piles, to simulate de-icing cycles, was 2.5 years with no signs of corrosion after that time. The findings supported the use of UNS# S31753 stainless steel alloy as prestressed strand material for concrete construction. That investigation was an excellent starting point for research into determining appropriate alloys for use as strand in prestressed concrete construction.

Later work by Sanchez[4] uses the work of Nürnberger as a starting point and expands upon those initial tests. Sanchez focused on the Arrhenius relationship between crack growth rate and inverse temperature as it relates to the onset of SCC in high-strength steels in a bicarbonate solution. At 25 ^{o}C, the crack growth rate was found to be 1.85E-09 m/s for cold drawn steel and 1.74E-09 m/s for modified parent pearlitic steel.

Later work by Moser[5] uses not only the work of Nürnberger, but many others as a basis for his work. Moser analyzed UNS # S30400, S31600, S31653, S32101, S32105, S32304 and S32205 and compared them using Slow Strain Rate Testing (SSRT) in varying concentrations of Cl^- to determine the best candidate high-strength stainless steel among those evaluated. The testing included both alkaline and carbonated solutions with Cl^- molar concentrations ranging from 0.25 to 1.0. The results showed pitting in the alloys with less Cr (S30400 and S32105) at lower Cl^- concentrations while S32205 showed the best corrosion resistance even in carbonated solution at 1.0M of Cl^-. Corrosion detected was in the form of pitting corrosion, with more pitting at either higher Cl^- concentrations or lower pH (Carbonated solution versus alkaline solution).

Further research is desired however to evaluate the performance of duplex stainless steel as well as manganese substitute austenitic stainless steels, given the increasing commercial availability of those materials as candidate alloys for this type of service. This investigation examined the SCC performance of a 300 series austenitic stainless steel alloy, a manganese substitute austenitic stainless steel alloy, and a duplex stainless steel. The temperature dependence of the time to cracking was in terms of an Arrhenius relationship. Anodic polarization was used and evaluated as an alternative test acceleration method.

EXPERIMENTAL PROCEDURE

Supplied Material Specifications

The three alloys tested were UNS# S31603, S24000, and S32205 (common names 316L, XM29 and 2205 respectively). The source for the material tested in these experiments was supplied by three manufacturing companies. The UNS# S31603 7-wire strand was supplied by National Strand Products Company[(2)] in Houston, TX, the UNS# S24000 7-wire strand was supplied by the Insteel Wire Products Company[(3)] in Sanderson, FL, and the UNS# S32205 single wire was supplied by Carpenter Steel (Carpenter Technology Corporation)[(4)] in Houston, TX.

The diameters of each alloy wire were as follows: 4.36 mm (0.171 inches) for UNS# S31603, 4.47 mm (0.178 inches) for UNS# S24000, and 4.56 mm (0.179 inches) for S32205. Their yield strengths as reported by the manufacturers were: 1.24 GPa (180 ksi) for UNS# S31603, 1.59 GPa (230 ksi) for UNS# S24000, and 1.59 GPa (230 ksi) for UNS# S32205.

The two main experimental methodologies used were designated as Phases 1 and 2 and are described in the following text. The polarization alternative testing was done as a separate evaluation from both phases and is also described below.

Phase 1 - Multiple Temperatures, $MgCl_2$ solutions.

In Phase 1, the supplied material was cut into segments 114 mm (4.5 inches) in length, unwound from a 7-wire strand to use only one of the wires from the strand (only for UNS# S31603 and UNS# S24000 as UNS# S32205 was supplied in a single wire form), and inserted into a three-point bending frame. As shown in Figure 1, an ~ 2 cm long portion of the wire length on the tension side (in the bending frame) was coated with Magnesium Chloride ($MgCl_2$) crystals that absorbed moisture from the test cell's airspace creating a mixture that was to remain saturated throughout the experiment. A wick was attached (using PTFE[(5)] tape) to the wire to ensure the solution stayed against the wire throughout the experiment. The three-point bending frame was placed in a small enclosure (12.5 cm long by 5.5 cm wide by 5.5 cm tall) (Figure 2) containing its own heating element and control thermocouple. The wire was then stressed by use of the three-point bending frame, and heated by a heating element underneath the frame.

The amount of stress applied to each specimen by the applied turns was calculated to be 1.15 GPa (167 ksi), 1.43 GPa (207 ksi) and 1.38 GPa (200 ksi) for the wires of alloy UNS# S31603, S24000 and S32205 respectively. This corresponds to 93%, 90%, and 87% of the yield strength of each alloy respectively.[6,7]

---

(2) Trade name.
(3) Trade name.
(4) Trade name.
(5) Trade name.

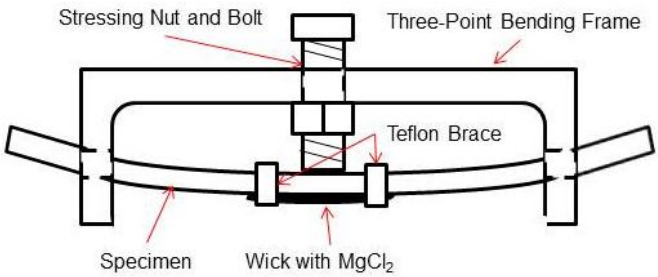

Figure 1 Diagram of Bending Frame

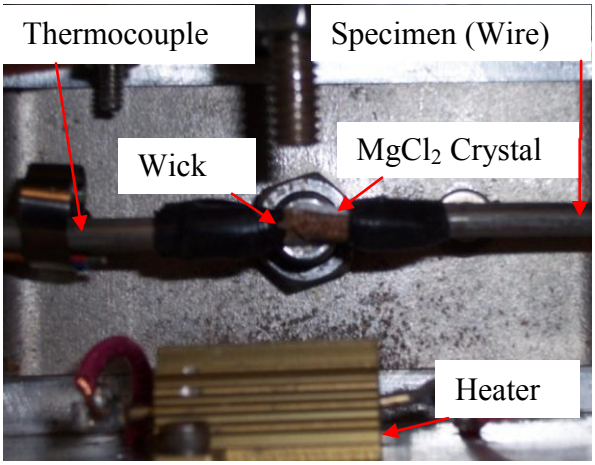

Figure 2 Small Enclosure (Bending Frame, Thermocouple, and Heater)

The small enclosure was in turn placed in the air space of a larger enclosure (Figure 3) that had deionized (DI) water placed at the bottom which was heated (by a heater underneath the large enclosure) to a temperature (T_1) corresponding to the water temperature needed for the Relative Humidity (RH) to be around 25% in the small enclosure. That RH level promoted the formation of a saturated $MgCl_2$ solution in the wick.

The temperature of the water in the large enclosure was controlled at its power supply. The large enclosure was sealed to minimize the loss of water and ensure the air space above the water was at the appropriate RH. The temperature of the wire (T_2) was measured by a thermocouple attached to the wire inside the small enclosure. This thermocouple output also controlled the heating element in the small enclosure through a process controller connected into the power loop of the heater. This setup caused the airspace in the small enclosure to be at a different RH (RH_2) than the rest of the large enclosure (RH_1).

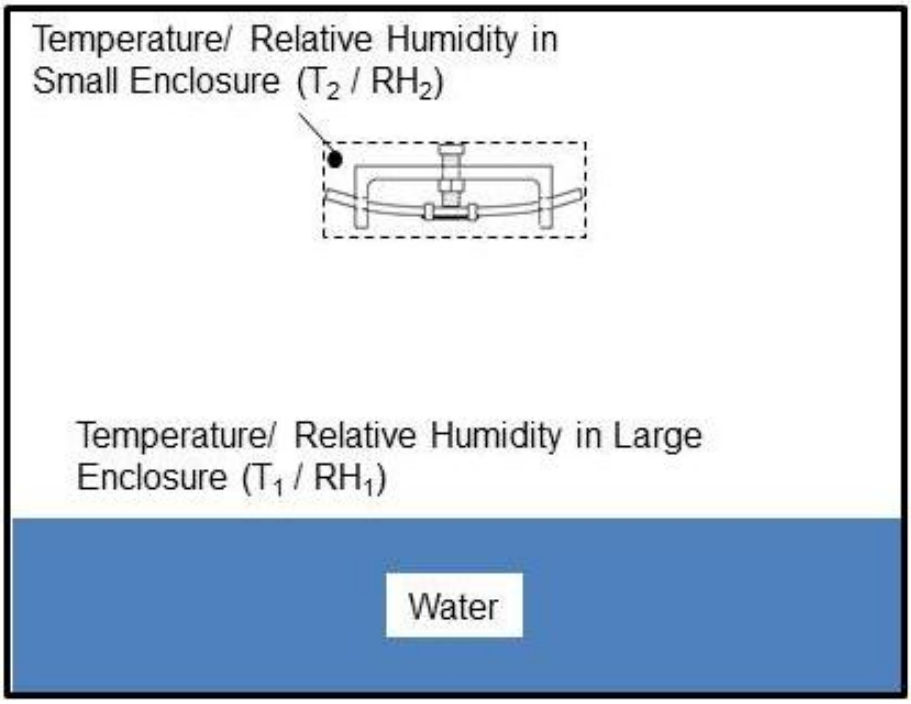

Figure 3 Diagram with Test Setup Process Parameters

Phase 2 - 60 ^{o}C, Simulated Concrete Pore Solution with Cl^-.

For phase 2, the alloys provided were cut down to 178 mm (7 inches), unwound in the case of UNS# S31603 and UNS# S24000 7-wire strand (Only the center wire was used for this phase). After cutting, the specimens were briefly (~< 1min) exposed to a 1 M nitric acid solution to clean off any low alloy steel particles that may have been embedded on the surface from the cutting process, degreased using ethanol, and rinsed with DI water. 6 specimens of each of the three alloys were tested in phase 2 (for a total of 18 specimens with specimens #1 through #6 being UNS# 31603, #7 through #12 being UNS# S24000 and #13 through #18 being UNS# S32205).

Once cleaned, each specimen was placed in a bending jig, and bent into a “U” bend. Stainless steel plates then placed onto the specimens to hold to them in the “U” bend (Figure 4a).

Measurements of the amount of springback each specimen displayed after bending were taken prior to being placed into the test chamber. These measurements provided an additional way by which to determine if SCC occurred in the specimens and not just pitting corrosion. If the specimen after testing did not springback as much as before the test, then this reduction in springback would be a sign that the material has experienced cracking

The potentials of each of the 18 specimens were recorded using an activated titanium reference (ATR) electrode (periodically calibarated agains a saturated calomel electrode (SCE)) that was permanently placed in the solution and wire connections to each of the specimens through the air-tight fittings in the test chamber wall, to a connector box with ports for each specimens. A significant drop in the potential of a specimens is indicative of corrosion occurring in that specimen. As this method of detection does not discriminate between types of corrosion, an secondary method of determining if the corrosion is SCC needs to be used.

For phase 2, specimens of each type of stainless steel were placed in a large container (12 inches inside diameter and 15 ½ inches tall) in a solution that contains 15% by weight Cl^- (adding NaCl to the solution in a sufficient quantity to reach that level of Cl^-), NaOH, KOH, $Ca(OH)_2$, and pure water to

simulate concrete pore water.[8, 9, 10] The simulated pore water solution (SPS) was created following the base solution composition shown in Table 1.

Table 1 Target Base Solution Composition for 15 wt% Cl and SPS Solution[11]

Chemical Composition (g/L) and pH Values of Model Solutions

	$Ca(OH)_2$[A]	NaOH	KOH[B]	Na_2CO_3	$NaHCO_3$	pH[C]	pH[D]
SCS	2.0	—	—	—	—	12.6	12.0
SPS	2.0	8.33	23.3	—	—	13.6	13.0
CPA	—	—	—	4.21	2.66	9.7	8.6

[A] Most of the $Ca(OH)_2$ was not dissolved.
[B] Reagent-grade KOH had a purity of only 85.3%.
[C] Before addition of Cl^-.
[D] With 15% Cl^-.

Therefore, 8.33 g of NaOH, 23.3 g of KOH, and 2 g of Ca $(OH)_2$ were added per liter of solution desired (per Table 1). NaCl was added to obtain a final 15% by weight Cl^- content. The solution had pH between 13 and 13.5. As the SPS solution when exposed to atmospheric conditions tends to drop in pH especially at higher temperatures (due to carbonation), the testing chamber was sealed with a gasketed lid to minimize the interaction with atmospheric CO_2 and possible decrease of pH as a result. Periodic pH measurements confirmed that it remained above 13 throughout the test.

A process controller maintained the temperature of the solution within the container typicallly within 5 °C of the target value (60°C). Two calibrated thermocouples were placed in two different points of the solution to ensure uniform temperature measurements of the solution. All wires for potential and temperature measurements went through air-tight fittings in the wall of the enclosure to maintain the air-tight seal. The entire setup was externally insulated to assist in maintaining temperature uniformity inside the test cell and is shown in Figures 4b and 5.

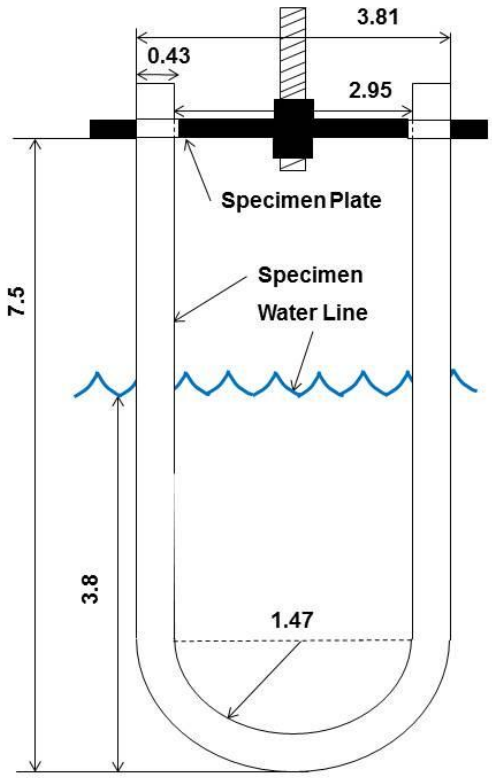

Figure 4a U-Bend Specimen Configuration (Units are in centimeters)

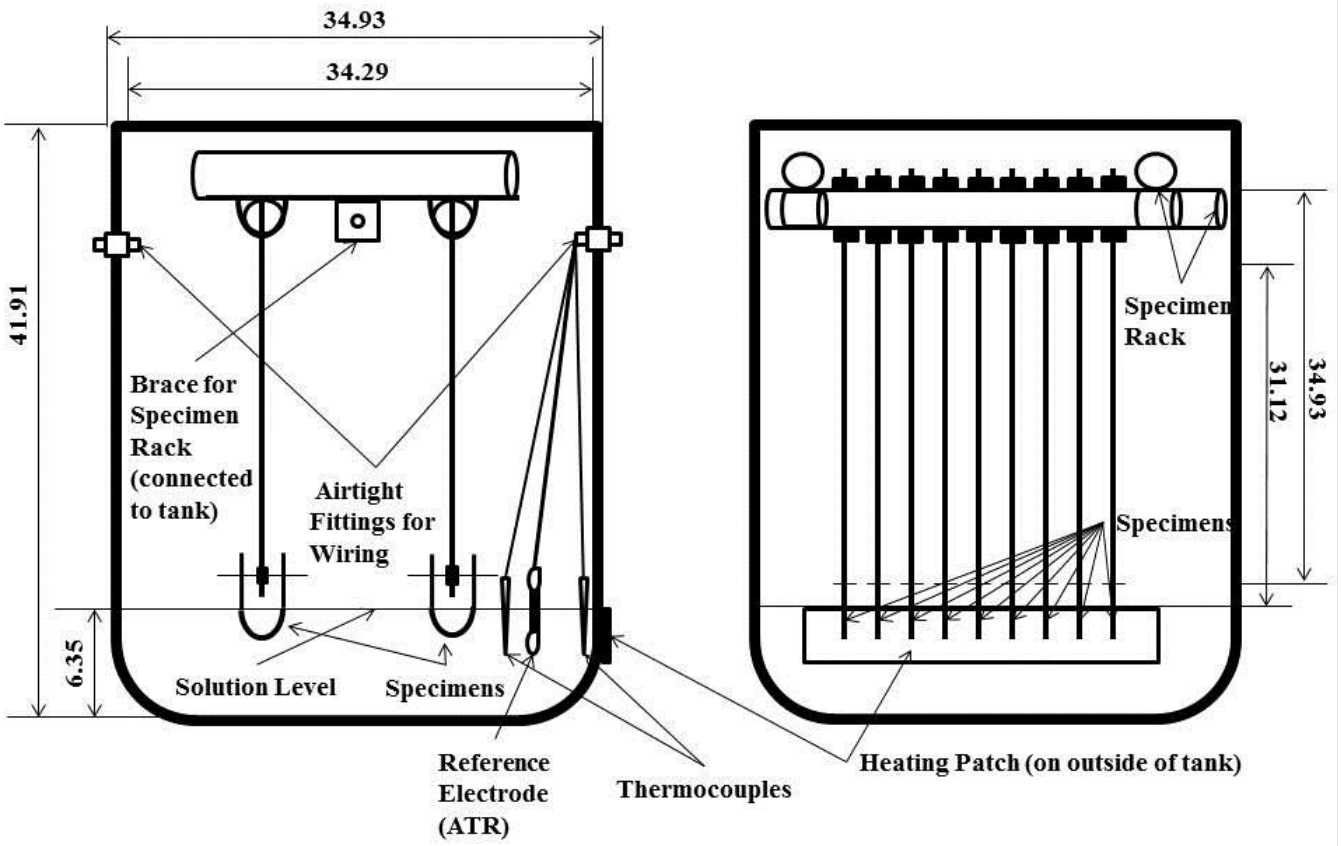

Figure 4b Diagram of Phase 2 Setup (Units are in centimeters)

Figure 5 Picture of Phase 2 Setup

Anodic Polarization of Selected Specimens from Phase 2

After 2160 hours of testing in phase 2, anodic polarization was imposed on select specimens using a multiple potentiostatic device. The objective of the increased polarization was to act as a test accelerator to induce SCC directly or by promotting pitting that then would increase local stress intensity and initiate cracking. Three specimens of each type of alloy were polarized to a potential that was 100 mV higher than the average OCP recorded shortly beforehand for each individual specimen. After 1900 hours of polarization, the polarization was increased an additional 100 mV. After 2000 hours at the higher potential, the polarization was increased again by 100 mV. Finally, after 1300 hours at the new higher potential, the polarization was increased yet again (to 400 mV higher than the initial OCP), and the specimens exposed for an additional 2200 hours.

RESULTS AND DISCUSSION

Phase 1

Figure 6 summarizes the results of the tests done on all three alloys. An SCC cracking event was declared if cracks were observed on the surface of the specimen by magnified visual inspection at the time of experiment conclusion. If no cracks were visually apparent in the specimens while still placed in the stressing frame, the specimen was removed, bent further to a hairpin shape with an inner radius of ~ 7 mm and examined again. If cracks were visible in that condition an SCC event was declared as well. A not-cracked event was declared otherwise.

SCC occurred in all three alloys tested. Only alloy UNS# S31603 experienced cracks at 60 ^{o}C (140 ^{o}F). Some data was offset left and right for display clarity. Sloping lines indicate Arrhenius abstraction of the results using estimated activation energies (Q). Estimating Q was performed by using a time for cracking assigned as the halfway point between the earliest crack observation and the latest no-crack condition. The data obtained allows estimation of an apparent activation energy for UNS# S31603 and UNS# S24000, Q ~ 72 kJ/mol (left green line) and ~ 81 kJ/mol (right red line), respectively. Those values are in rough agreement with temperature dependence properties of SCC reported in the literature.[11] The quantity of data for alloy UNS# S32205 was not sufficient to establish a crack-no crack transition so one was established only at 90 ^{o}C (194 ^{o}F). The middle dotted line was traced using the working assumption that Q for that material was comparable to that of UNS# S31603 and UNS# S24000. Nominal time to SCC at 40^{o}C is obtained for each material by extrapolation. The 10 year and 100 year markers are shown for contrast. Extrapolation of those trends would suggest that at 40 ^{o}C (an estimated service temperature extreme for prestressed piles) cracking time would be in the order of one week for UNS# S31603, a few years for UNS# S32205, and 80 plus years for the UNS# S24000. In this test, UNS# S24000 performed the best followed by S32205 and lastly UNS# S31603.

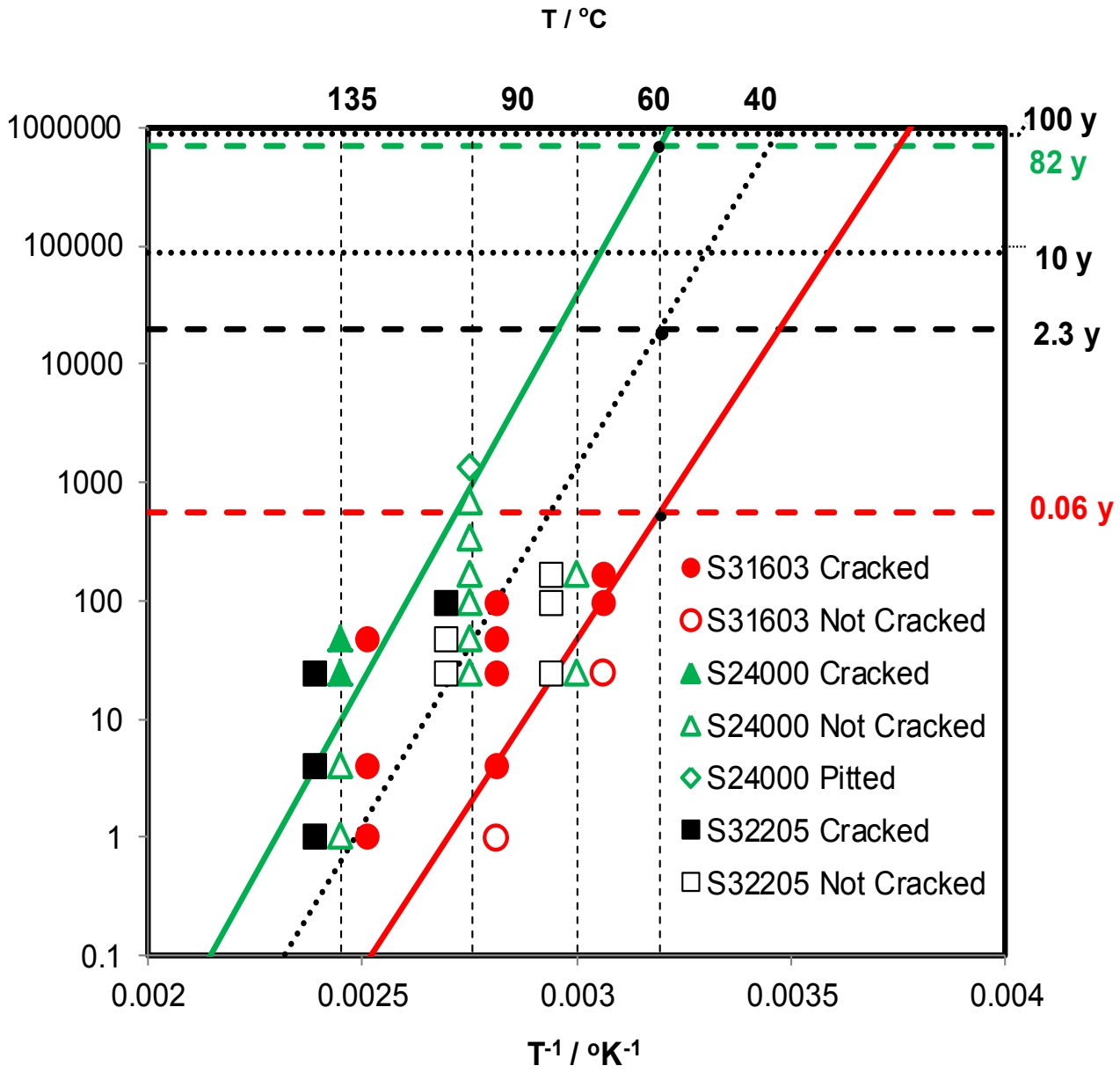

Figure 6 Graph of Exposure Time (Log Scale) indicating Test Outcome, as Function of Inverse Absolute Temperature

One indicator that SCC has occurred rather than another form of corrosion or mechanical failure is the branching of cracks that lead to failure. Branching cracks that are transgranular are a clear sign that the failure mechanism was SCC rather than failure due to pitting corrosion causing the loss of cross section, for example. Figures 7a, 7b, and 7c show the surface cracks (circled for clarity) on a specimen of UNS# S31603 tested at 60 °C for 168 hours, a specimen of UNS# S24000 tested at 90 °C for 1344 hours, and a specimen of UNS# S32205 tested at 135 °C for 1 hour. Figures 8a, 8b, and 8c show the metallographic cross-sections of those specimens with branching cracks that cut across the grain boundaries (the grains are stretched into thin strips due to the cold working process, with the drawing direction vertical for Figures 8a, 8b, and 8c and as shown clearly in Figure 8c).

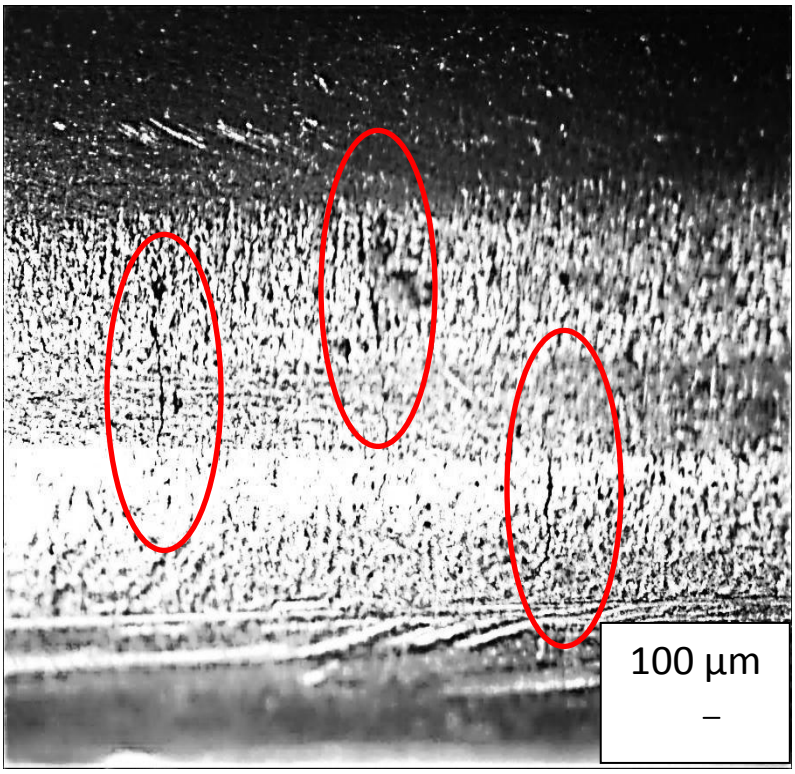

Figure 7a Picture of SCC at Surface of Cracked UNS# S31603Specimen - Phase 1

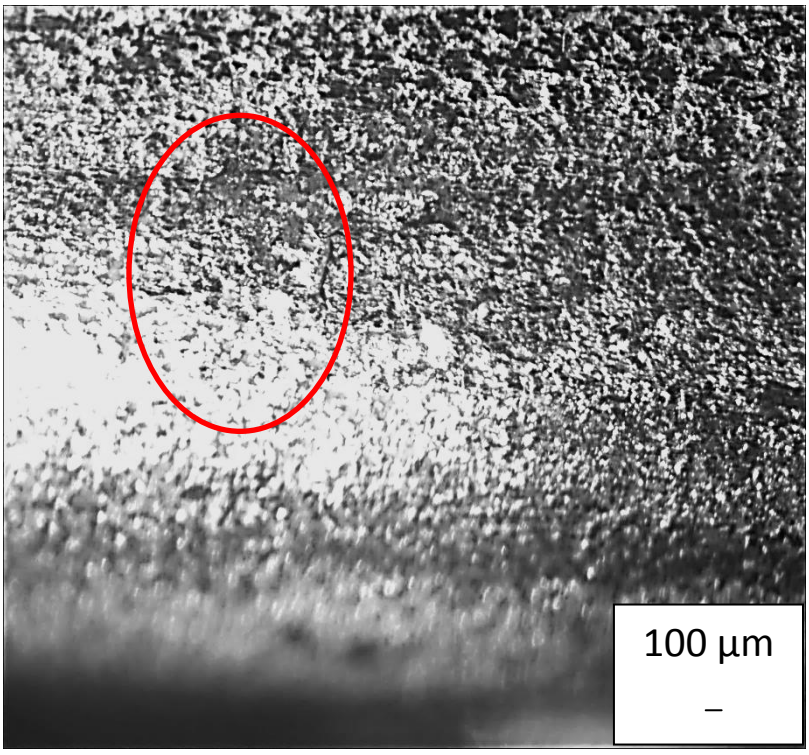

Figure 7b Picture of SCC at Surface of Cracked UNS # S24000 Specimen - Phase 1

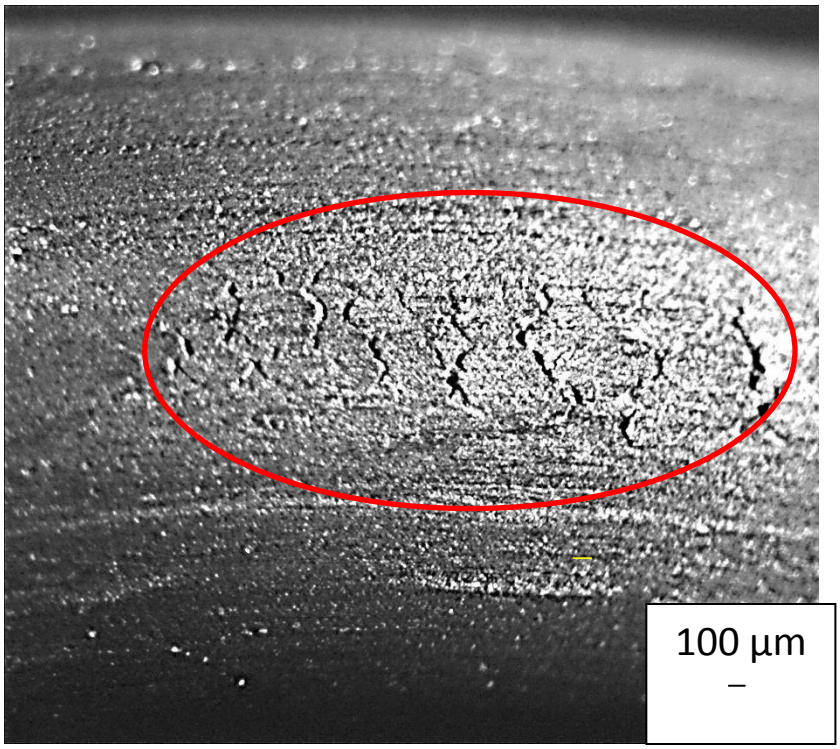

Figure 7c Picture of SCC at Surface of Cracked UNS # S32205 Specimen - Phase 1

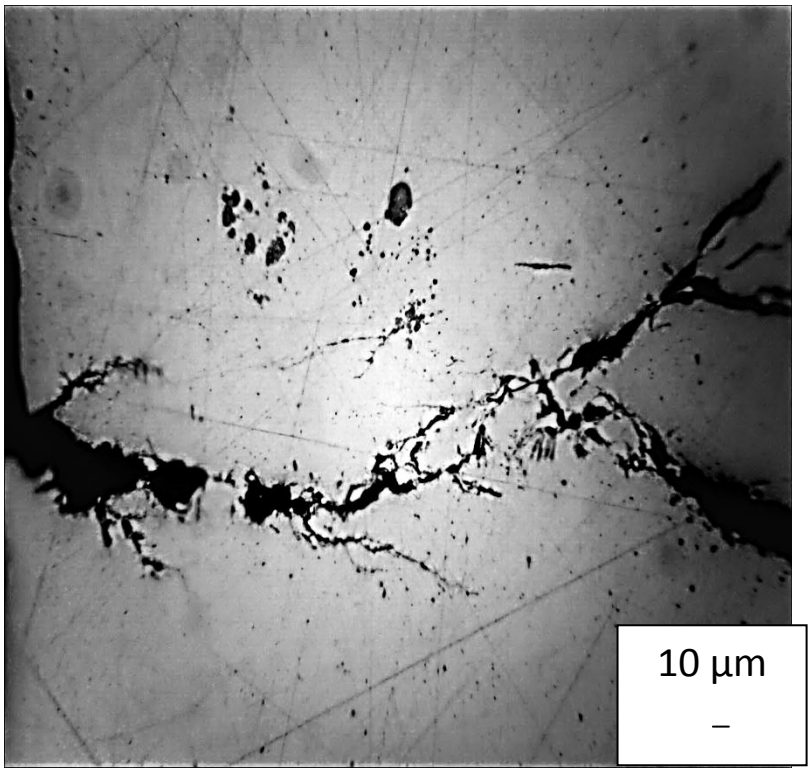

Figure 8a Metallographic Cross-Section of Cracked UNS# S31603 Specimen - Phase 1

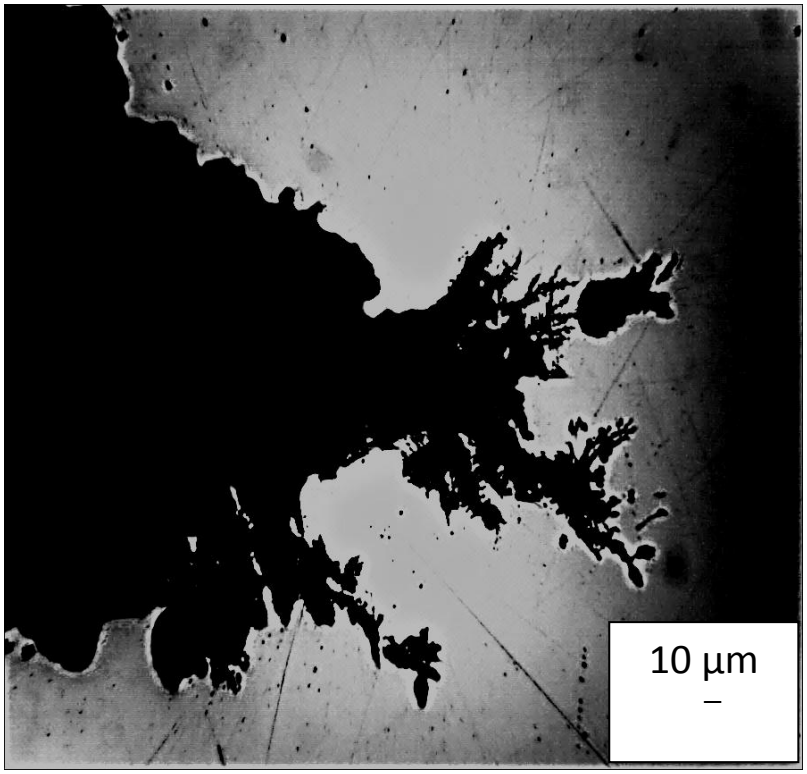

Figure 8b Metallographic Cross-Section of Cracked UNS# S24000 Specimen - Phase1

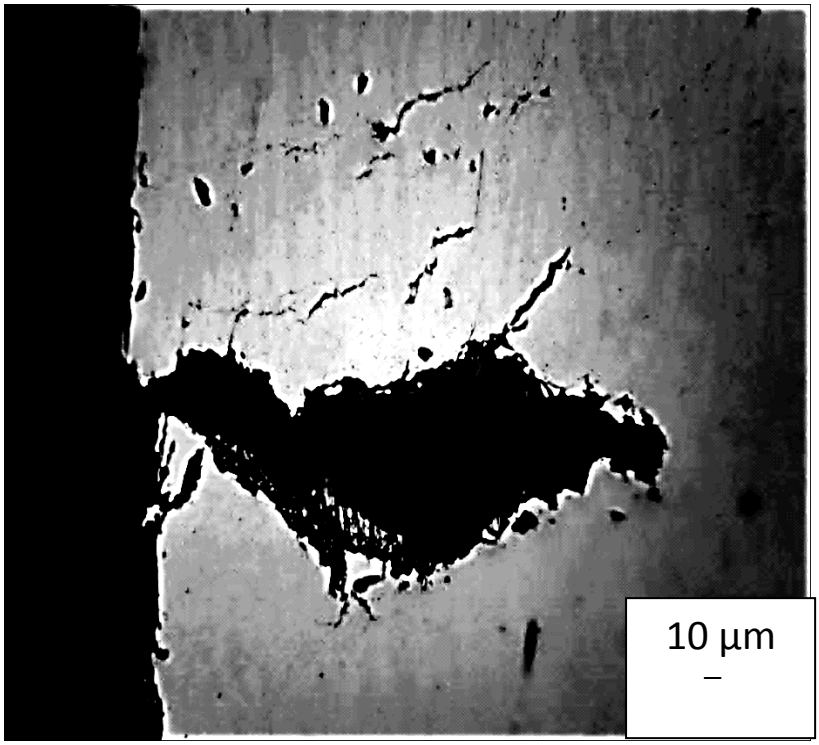

Figure 8c Metallographic Cross-Section of Cracked UNS# S32205 Specimen (The austenitic phase are shown as the light regions while the ferritic phase as the dark regions) - Phase 1

Phase 2 - Initial Stage

Figure 9 displays as function of time the potential range (highest and lowest valued) measured in the multiple specimens of each alloy evaluated for the initial 2160 h test period. This display form is used for clarity given the large number of specimens involved. None of the specimens of any alloy (18 specimens total) showed signs of corrosion after 2160 hours. None of the potentials dropped to below -300 mV versus SCE, and most potentials stayed under -100 mV versus SCE. All alloys performed equally well in this stage of the test.

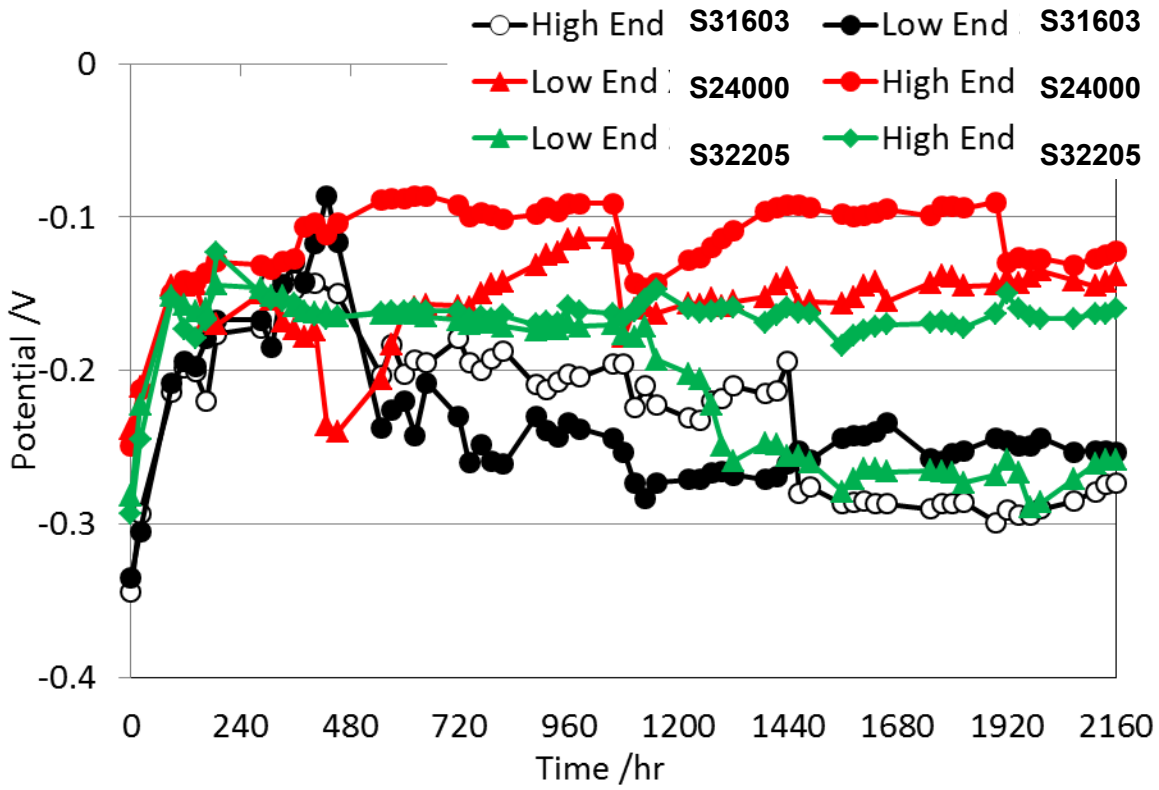

Figure 9 Potential (SCE scale) versus Time during Phase 2 tests at 60°C (140 °F) for UNS# S31603, S24000, and S32205. Initial 2160 hour stage. Specimens #1 through #18.

Phase 2 - Subsequent Anodic Polarization of Selected Specimens

Table 2 summarizes the data obtained during the polarization stage of the test. 9 of the 18 specimens from phase 2 were polarized, and only 2 of those 9 (both UNS# S32205 alloy specimens) did not experience pitting or SCC during the polarization time period. Two of the UNS# S24000 specimens (specimens #10 and #11) failed at +100 mV over the initial OCP (IOCP), while the third UNS# S24000 specimen failed at +200 mV over IOCP. All three specimens of UNS# S31603 failed at +300 mV over IOCP, with specimen #6 left in for ~2.5 weeks following the initial sign of corrosion. After those ~2.5 weeks, specimen #6 showed clear signs of SCC, while its initial corrosion indication by a spike in the current demand showed only signs of pitting at that time. The pitting evolving into SCC as shown by this specimen confirmed as expected that pitting promotes SCC and that propensity for pitting should be then considered as a derating factor in assessing the susceptibility to SCC of a particular alloy. Only specimen #16 of alloy UNS# S32205 failed, and that failure started as pitting and was allowed to continue (for ~3.5 weeks) to the stage of SCC at +400 mV over IOCP. In summary, one UNS# S32205 specimen failed only at the highest polarization of +400 mV over IOCP while all three UNS# S31603 specimens failed at +300 mV over IOCP. All three UNS# S24000 specimens failed at or below +200

mV over IOCP polarization, showing that this alloy had the poorest performance in this test. Therefore, UNS# S32205 is considered to have performed better in this test as compared to UNS# S24000 and S31603.

A clear indicator of fully developed SCC as opposed to just precursory pitting in these specimens was loss of springback. Significant percentage of springback loss (~ 30% and above) was deemed to indicate that the specimen has experienced SCC. If there were visual signs of pitting, but the percentage of springback loss was below 30%, only pitting corrosion was deemed to have occurred. It is noted that due to minor measurement uncertainty, some specimens showed negative loss of relaxation, but the effect was small as compared to the differences of springback in failed specimens.

Table 2
Results of Polarization of Select Specimens of Phase 2 and Percent Difference from Initial to Final Bent and Relaxed Values.

Specimen # / Alloy UNS#	Final Condition	Percent Difference from Initial Value to Final Value Relaxed (%)
#2 / S31603	Pitting	-0.79%
#4 / S31603	Pitting	-1.43%
#6 / S31603	SCC	30.32%
#8 / S24000	Pitting	5.87%
#10 / S24000	SCC	48.89%
#11 / S24000	SCC	50.63%
#16 / S32205	SCC[(A)]	18.69%
#17 / S32205	No Pitting /SCC	-16.26%
#18 / S32205	No Pitting /SCC	-1.87%

[(A)] Note: specimen experienced severe deformation from "U"-bend shape.

CONCLUSION

The results suggest that duplex high-strength stainless steel UNS# S32205 performed overall better than the other two alloys. While UNS# S32205 performed second best in the Phase 1 tests, it had clearly superior performance in the Phase 2, anodic polarization stage tests, which involved high severity and were also conducted in an environment more representative of conditions in concrete. The results of testing in the initial stage of Phase 2 was nevertheless encouraging in that none of the three alloys exhibited any signs of SCC in an environment that simulated heavily Cl- contaminated concrete pore water at a highly accelerating temperature regime. These findings are preliminary in nature and should be supplemented by the results of longer time exposures.

ACKNOWLEDGEMENTS

The author thanks the Florida Department of Transportation for their financial support of this study (The opinions, findings, and conclusions expressed here are those of the author and not necessarily those of any supporting organization).

REFERENCES

1 A. Sagüés, S.C. Kranc, F. Presuel-Moreno, D. Rey, A. Torres-Acosta, L. Yao, “Corrosion Forecasting for 75-Year Durability Design of Reinforced Concrete”, Florida Department of Transportation Final Report BA502 (located at http://www.dot.state.fl.us), December 2001.

2 W. H. Hartt, R. G. Powers, V. Leroux, and D. K. Lysogorski, “A Critical Literature Review of High-Performance Corrosion Reinforcement in Concrete Bridge Applications”, Federal Highway Administration Report, FHWA-HRT-04-093 (located at http://www.fhwa.dot.gov), July 2004.

3 Y. Wu and U. Nürnberger, “Corrosion-technical Properties of High-Strength Stainless Steels for the Application in Prestressed Concrete Structures”, Materials and Corrosion, Volume 60, Number 10, p. 771-780, 2009

4 J. Sanchez, J. Fullea, and C. Andrade, “Stress Corrosion Cracking Mechanism of Prestressing Steels in Bicarbonate Solutions”, Advances in Construction Materials, Part V, Pages 397-404, 2007.

5 R. Moser, “High-Strength Stainless Steels for Corrosion Mitigation in Prestressed Concrete: Development and Evaluation”, A Dissertation at Georgia Institute of Technology, August 2011.

6 “Product Data Bulletin - Hot-Rolled Steel”, Product Catalog Sheet from AK Steel Corporation, 2007.

7 J.R. Davis , “ASM Specialty Handbook Stainless Steels”, ASM International, Materials Park, OH, December 1994.

8 F. Cui and A. Sagüés , "Exploratory Assessment of Corrosion Behavior of Stainless Steel Clad Rebar", Corrosion, Volume 62 No. 9, Pages 822-838, September 2006.

9 T. Baumeister and Lionel Marks, “Standard Handbook for Mechanical Engineers”, 7th Edition, McGraw-Hill, New York, NY, 1958.

10 Robert C. Weast, “Handbook of Chemistry and Physics”, 54th Edition, Published by CRC Press, Boca Raton, FL, 1973-1974.

11 J. Fernandez, “Stress Corrosion Cracking Evaluation of Candidate High Strength Stainless Steels for Prestressed Concrete”, University of South Florida, Tampa, FL, December 2011.

12 O. M, Alyousif and R. Nishimura, “The Effect of Test Temperature on SCC Behavior of Austenitic Stainless Steels in Boiling Saturated Magnesium Chloride Solution”, Corrosion Science, Volume 48, Pages 4283-4293, May 2006.